Role of Gallium Doping in Dramatically Lowering Amorphous-Oxide Processing Temperatures for Solution-Derived Indium Zinc Oxide Thin-Film Transistors

By *Sunho Jeong, Young-Geun Ha, Jooho Moon, Antonio Facchetti,** and *Tobin J. Marks**

Amorphous-oxide semiconductors (AOSs) are promising candidates as transparent semiconductors for thin-film transistor (TFT) circuitry due to their favorable field-effect mobilities, excellent environmental/thermal stability, high optical transparency, and potential for low-temperature film processing.[1] In AOS materials, the conduction band minimum (CBM), which constitutes the electron conduction pathway, is composed of vacant metal cation s-states. When the spatial expanse of these s-states is greater than the intercation distances, AOSs exhibit electron mobilities comparable to those of the corresponding crystalline phase(s).[1a,2] The s-state spatial overlap is primarily determined by the principal quantum number (n) and, therefore, heavy post-transition metal cations with $(n-1)d^{10}ns^0$ electronic configurations, where $n \geq 5$, are ideal AOS candidates. Both In^{3+} and Sn^{4+}, with the same $[Kr](4d)^{10}(5s)^0$ electronic configuration, meet this requirement. A highly dispersed CBM is also found in ZnO due to the small intercation distances.[2b,3] The mixing of different-sized aliovalent cations is effective in enhancing amorphization,[4] so that AOSs with stable amorphous phases are formed in both binary and ternary AOS compositions.

To date, amorphous indium zinc oxide (IZO), zinc tin oxide (ZTO), zinc indium tin oxide (ZITO), and indium gallium zinc oxide (IGZO) thin films have been grown, primarily using vacuum-based physical-vapor-deposition techniques. TFTs based on these materials exhibit electron mobilities $>10\,cm^2\,V^{-1}\,s^{-1}$, even for film growth near room temperature.[1a,5] While these AOSs offer promise as emerging materials for the realization of transparent TFTs and unconventional electronic device applications,[6] reliance on vacuum-based processes significantly increases manufacturing costs and poses major obstacles for realizing modern large-area, inexpensive electronics. In contrast, solution deposition of semiconductors offers many advantages such as equipment simplicity, low cost, and high throughput. Recently, several groups have explored solution techniques for growing TFT-quality AOS films and, in several cases, electron mobilities $>10\,cm^2\,V^{-1}\,s^{-1}$ were reported for IZO- and ZTO-based transistors.[7] However, these high mobilities were obtained only when the oxide films were annealed at temperatures typically >500 °C. At 400 °C, mobilities fall by ~10× and, below 400 °C, no TFT function is observed.[7a,b]

In contrast to Sn-, In-, and Zn-based films, solution-processed Ga-doped AOS films have barely been investigated. For vacuum-deposited AOS films, Ga has been used to reduce doping sensitivity to the O_2 partial pressure.[8] Since Ga–O bonding is far stronger than either Zn–O or In–O bonding, charge-carrier generation via formation of oxygen vacancies is more demanding. On the other hand, since solution-processed AOS films are typically annealed in ambient conditions to thermally decompose the metal-oxide precursors and by-products, the dependence of transistor performance on the O_2 partial pressure should not be a major concern. In principle, Ga doping of solution-processed AOSs may decrease mobility because the lack of oxygen vacancies prevents prefilling of trap states. Recently, Kim et al., reported solution-processed IGZO films, however, they deliberately adjusted the composition to obtain the crystalline phase by annealing above 400 °C and focused how the In^{+3} concentration influences the ultimate film crystallinity and electrical properties.[9] In this study, we report novel solution-processed amorphous Ga-doped IZO films and demonstrate the key, heretofore unrecognized role of Ga in enabling low-temperature TFT film processing. The electrical characteristics of TFTs based on IZO, IGZO, and GZO films are compared and contrasted to elucidate the effects of structure, annealing temperature, and metal composition on TFT-performance parameters.

Bottom-gate/top-contact TFTs were fabricated on heavily doped p^{++}-Si/(300 nm) SiO_2 substrates by spin-coating IZO, IGZO, or GZO precursor solutions (see the Experimental section for details). The resulting films were annealed at temperatures ranging from 400 °C to as low as 250 °C. The amorphous nature of all films was confirmed by grazing angle XRD measurements

[*] Prof. T. J. Marks, Dr. A. Facchetti, Dr. S. Jeong,[+] Y.-G. Ha
Department of Chemistry and the Materials Research Center
Northwestern University
2145 Sheridan Road, Evanston, IL 60208 (USA)
E-mail: t-marks@northwestern.edu; a-facchetti@northwestern.edu
Prof. J. Moon
Department of Materials Science and Engineering
Yonsei University
134 Shinchon-dong, Seodaemun-gu, Seoul 120-749 (Korea)
[+] Present address: Korea Research Institute of Chemical Technology, 19 Sinseongno, Yuseong, Daejeon 305-600 (Korea)

DOI: 10.1002/adma.200902450

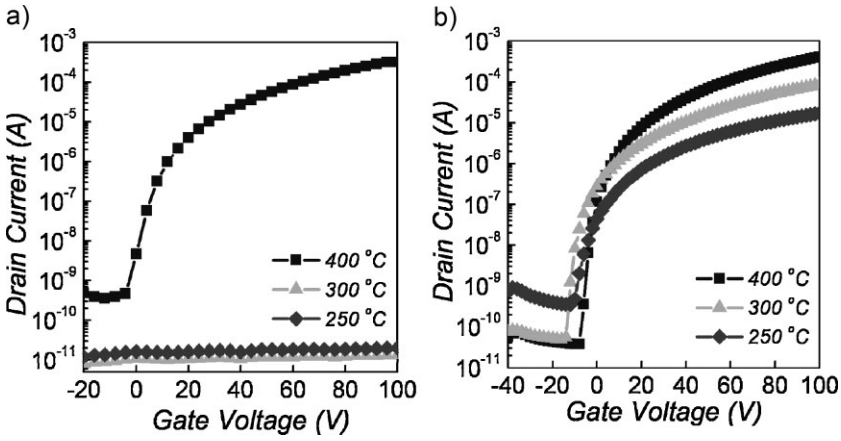

Figure 1. Transfer characteristics of transistors based on IZO (a) and IGZO (b) films annealed at the indicated temperatures from 250 to 400 °C. The chemical composition ratio for IZO and IGZO is In:Zn = 70:30 and In:Ga:Zn = 63:10:27, respectively. The applied drain voltage is 100 V.

(see the Supporting Information, Fig. S1). TFT fabrication was completed by thermal evaporation of Al source and drain contacts through a shadow mask. Figure 1 shows representative transfer characteristics for TFTs based on IZO (In:Zn = 70:30) and IGZO (In:Ga:Zn = 63:10:27) films. The output characteristics for an optimized IGZO-based TFT are shown in Figure S2 (Supporting Information). The TFT performance parameters, including the field-effect mobility (μ), the threshold voltage (V_T), the on-current (I_{on}), and the on-to-off current ratio ($I_{on/off}$) are summarized in Table 1. TFTs based on IZO and IGZO film annealed at 400 °C exhibit good field-effect characteristics with $\mu \sim 1\,cm^2\ V^{-1}\ s^{-1}$.

Table 1. Electrical-performance parameters of transistors (carrier mobility calculated in saturation, ±15%) fabricated from IGZO films having different In:Zn ratios as well as IZO and GZO. The composition ratio of the IZO and GZO precursor solutions is In:Zn = 70:30 and Ga:Zn = 10:90, respectively. The composition ratio of the IGZO precursor solution was varied over a molar ratio of In:Ga:Zn = *x*:10:(90–*x*).

	In [mol%]	Temperature [°C]	μ [$cm^2\ V^{-1}\ s^{-1}$]	V_T [V]	*Ion* [A]	*Ion*/off
IZO	70	400	1.0	18.7	3×10^{-4}	10^6
		300		inactive		
		250		inactive		
IGZO	68	400	1.54	−6.28	6.7×10^{-4}	8×10^6
		300	0.4	5.6	1.3×10^{-4}	4×10^6
		250	0.008	14.6	2.8×10^{-6}	5×10^4
	63	400	1.1	25.3	3.5×10^{-4}	6×10^6
		300	0.2	12.8	8×10^{-5}	5×10^5
		250	0.05	−1.3	2×10^{-5}	10^5
	58	400	0.85	17	2.4×10^{-4}	10^6
		300	0.08	21	3×10^{-5}	3×10^5
		250	0.006	43.7	9×10^{-7}	4×10^4
	23	400	0.2	14	5×10^{-5}	10^6
		300	0.02	32	5×10^{-6}	3×10^4
		250	0.002	53.2	2.6×10^{-7}	7×10^3
GZO	0	400	0.006	40.6	1×10^{-6}	10^4
		300	0.0009	58	9×10^{-8}	10^3
		250	0.0002	64.6	1.5×10^{-8}	5×10^2

However, whereas IGZO-based TFTs operate well when the semiconductor films are annealed at 300 °C ($\mu \sim 0.2\,cm^2\ V^{-1}\ s^{-1}$) and 250 °C ($\mu \sim 0.05\,cm^2\ V^{-1}\ s^{-1}$), the corresponding IZO-based TFTs are inactive. The low drain current for IGZO-based TFTs annealed at 250 °C is not affected by the gate leakage current, since the leakage current through the gate dielectric is lower than the drain current by a factor of 100. This result indicates that Ga doping enables active TFTs based on solution-processed low-temperature-annealed AOS films. To understand these mobility trends, the chemical and structural evolution of the IGZO films with the film-annealing temperature were analyzed by X-ray photoelectron spectroscopy (XPS). Figure 2 shows O1s XPS spectra for IZO and IGZO films annealed at the indicated temperatures. The peaks centered at ~529.9 and ~531.4 eV can be assigned to oxygen in oxide lattices without oxygen vacancies and with oxygen vacancies, respectively.[10]

Lower electron density reduces screening effects on the nuclei, which raises the effective nuclear charge. The feature at ~531.7 eV can be assigned to the oxygen in hydroxide.[5a,10c] Since H is more electronegative than the metals (In, Ga, Zn), the M−OH oxygen atoms are less negatively charged than those in oxides, shifting the

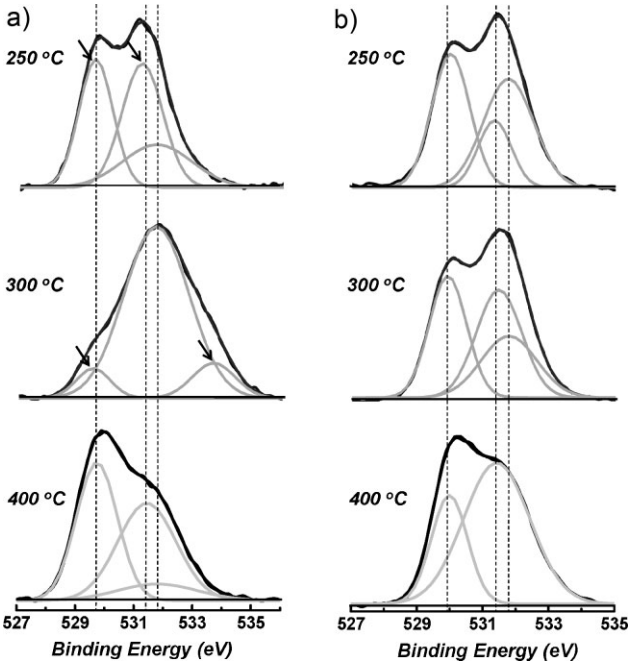

Figure 2. O1s XPS spectra for IZO (a) and IGZO (b) films annealed at the indicated temperatures. The composition ratio of IZO and IGZO precursor solutions is In:Zn = 70:30 and In:Ga:Zn = 63:10:27, respectively. The dashed lines indicate peaks that originate from oxide lattices without oxygen vacancies (~529.9 eV), oxide lattice with oxygen vacancies (~531.4 eV), and hydroxide (~531.7 eV), respectively. The arrows indicate the unassigned peaks discussed in the text.

XPS feature toward higher binding energy. The XPS data indicate that the IZO films annealed at 400 °C contain small amounts of metal hydroxide and both types of oxide lattice. For solution-processed metal-oxide-semiconductor films, metal hydroxides are gradually converted into the oxides via thermally-driven condensation processes and the degree of oxide-lattice formation and oxygen-vacancy generation depends, for a given composition, primarily on the annealing temperature. Note that the IZO films annealed below 300 °C are composed primarily of hydroxides. The unassigned XPS peaks (arrows in Fig. 2) probably originate from intermediate compounds due to incomplete metal-precursor-to-hydroxide conversion. In contrast to these results, IGZO films annealed at 400 °C consist of oxide lattices with minimal hydroxide content and oxide lattices persist even when the film is annealed below 300 °C. Importantly, as shown in Figure 3a, Ga doping allows the amorphous-oxide semiconductors to achieve oxide-lattice structures at far lower temperatures.

The conduction band minimum in AOSs should be primarily composed of dispersed vacant s-states with short intercation distances for efficient carrier transport, which can be achieved in ionic oxide lattices but not so obviously in hydroxide lattices. Therefore, it is reasonable that metal-oxide-lattice formation is an essential prerequisite for low-temperature-annealed amorphous semiconducting films with good mobilities. This is in accord with the aforementioned observations that TFTs based on IZO films annealed below 300 °C are inactive, while TFTs based on IGZO films annealed below 300 °C function well.

The XPS data also allow semiquantitative analysis of the oxygen-containing species and suggest that the relative concentration of oxygen vacancies within IGZO films decreases by ~4.1× as the annealing temperature decreases (Figure 3b). The oxygen-vacancy formation process closely relates to the generation of charge carriers, according to Equation (1).

$$O_o^x = \frac{1}{2}O_{2(g)} + V_o^{\bullet\bullet} + 2e^- \quad (1)$$

Here, O_2 is lost from the oxide sublattice (O_o^x) to create a doubly charged oxygen vacancy ($V_o^{\bullet\bullet}$) and two free electrons. It can be presumed that IGZO films annealed at higher temperature attain more charge carriers due to thermally enhanced oxygen-vacancy formation processes. It has been reported that the mobility of amorphous IGZO films depends on the carrier concentration, since the carrier transport is governed by percolation conduction over trap states and is enhanced at high carrier concentrations by filling the trap states.[1a,11] Therefore, the decrease in carrier mobility for low annealing temperatures can be attributed to a decrease in oxygen vacancies.

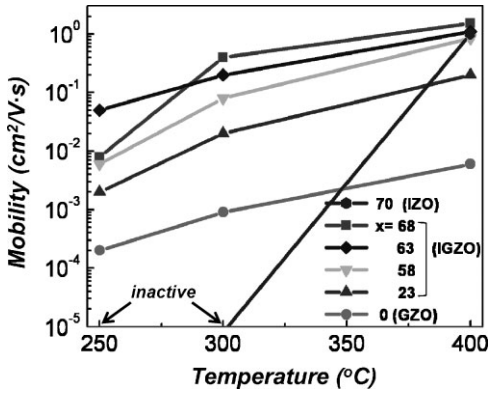

Figure 4. Field-effect electron mobilities of transistors based on IGZO films with the indicated In compositions (In:Ga:Zn = *x*:10:(90–*x*)) as well as for IZO and GZO films.

We also analyzed the effects of metal composition in the present AOS films. Figure 4 shows mobility-versus-annealing-temperature and composition plots for TFTs based on IGZO films with different In contents as well as for IZO and GZO films. The electrical characteristics of these transistors are also summarized in Table 1. The field-effect mobilities decrease with decreasing annealing temperature, independent of composition. This result is in accord with the aforementioned thermally driven oxygen-vacancy formation process. For vacuum-deposited IGZO films it is known that the mobility is enhanced by increasing the In content due to the generation of more charge carriers.[12] This trend is also observed in the present solution-processed IGZO-based TFTs and the mobility increases by ~400× when the In content is increased from 0 to 63 mol%. However, further increases in In content abruptly decrease the mobility of IGZO films annealed at 250 °C. For AOSs based on In_2O_3 and ZnO, the spatial spread of vacant s-states is so large that direct overlap between the s-states of neighboring cations is possible. However, the intercation In···In and Zn···Zn distances are greater at low annealing temperatures, generating shallow localized states beneath the conduction band minima and, in turn, decreasing carrier mobility.[13a] These localized states are diminished by structural relaxation effects, which are accompanied by shortening of the intercation distances during annealing.[13] However, the In···In intercation distance is larger than that of Zn···Zn, so that In-rich IGZO films have higher threshold energies for structural relaxation. As a consequence, structural relaxation in In-rich IGZO films is incomplete at 250 °C, resulting in electron-low mobility. Regarding choice of host material for Ga doping, either tailoring the

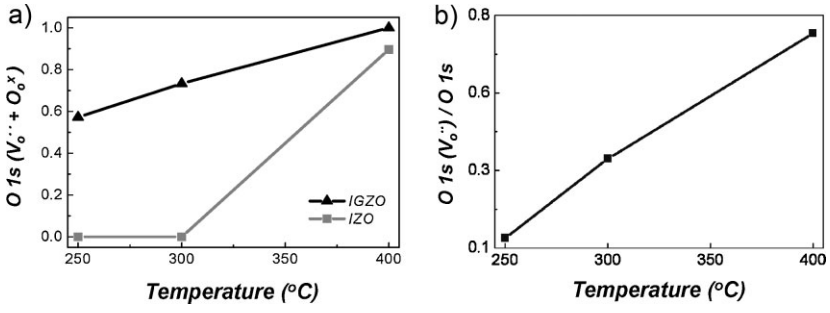

Figure 3. a) The fractions of oxide lattices in IZO and IGZO films and b) the relative concentrations of oxygen vacancies in IGZO films. All calculations are performed based on an area integration of each O1s peak. O1s (O_o^x) and O1s ($V_o^{\bullet\bullet}$) denote the O1s features due to oxide lattices without oxygen vacancies and with oxygen vacancies, respectively.

composition or selecting a metal cation that does not have low-temperature-annealing limitations should be considered.

In summary, we have developed a new solution-based, low-temperature annealing process for amorphous Ga-doped IZO films suitable for TFTs, complimenting the recent impressive results achieved with crystalline metal oxide semiconductors.[14] In doing so, we clarified some of the chemical requirements for the low-temperature solution processing of these oxide semiconductors, showing that oxide-lattice formation and the generation of sufficient charge carriers via oxygen-vacancy formation are essential for achieving acceptable TFT performance. We also demonstrated that In plays a significant role in enhancing electron mobility but, simultaneously, shows limitations in low-temperature annealing due to the larger intercation distances. Furthermore, the present novel Ga-based AOS synthetic pathway opens important possibilities for solution-processed and low-temperature annealed TFTs, and we foresee even higher field-effect mobilities with appropriate selection of oxide semiconductors for Ga doping and insulators for gate dielectrics.

Experimental

Precursor Solution Synthesis: The IZO, IGZO, and GZO precursor solutions were synthesized using zinc acetate dihydrate (98%), indium nitrate hydrate (99.9%), and gallium nitrate hydrate (99.9%). Solutions, 0.375 M in metal precursors, were prepared in 2-methoxyethanol (99%) with 0.87 M monoethanolamine (99%) as a stabilizer. All reagents were purchased from Aldrich Chemicals and were used without further purification. The chemical composition ratio of IGZO precursor solution was varied, with a molar ratio of In:Ga:Zn = x:10:(90–x), where x is the mole fraction of In precursor. The chemical composition ratio of IZO and GZO precursor solutions was In:Zn = 70:30 and Ga:Zn = 10:90, respectively. These clear solutions were stirred for 3 h at room temperature before spin-coating.

Transistor Fabrication and Electrical Performance Characterization: Doped silicon substrates with a 300-nm-thick thermal silicon dioxide layer, which are used as the gate dielectric, were sonicated with absolute ethanol and dried with an N_2 stream, followed by oxygen plasma treatment for 5 min. Subsequently, each precursor solution was spin-coated at 4000 rpm for 35 s and then annealed at 400 °C for 30 min. For the fabrication of transistors with a top-contact-electrode architecture, Al source and drain electrodes of 50 nm thickness were deposited by thermal evaporation (pressure $\sim 10^{-6}$ Torr) through shadow masks. The channel length and width are 100 and 1000 μm, respectively. TFT characterization was performed under ambient conditions using a Keithley 6430 Sub-Femtoamp Remote Source Meter and a Keithley 2400 Source Meter with a locally written *LABVIEW* program and general-purpose interface bus communcation. Saturation mobilities were extracted from the slope of (drain current)$^{1/2}$ versus gate voltage, derived from the device-transfer plot.

Film Characterization: The chemical and electronic structures of the oxide semiconductors were examined by XPS (Omicron, ESCA Probe). The surface XPS data were collected using monochromatic Al Kα radiation (1486.6 eV) in an ultrahigh-vacuum system with a base pressure of $\sim 10^{-10}$ Torr. The binding energy shift was corrected using the C1s peak. The crystal structures were identified by grazing angle XRD using Cu Kα radiation on a Rigaku ATX-G Thin-Film Diffraction Workstation.

Acknowledgements

We thank Polyera Corp. and the US-Israel BSF for support of this research and the Northwestern MRSEC (NSF DMR-0520513) for characterization facilities. This work is also partially supported by a Korea Research Foundation Grant funded by the Korean Government [KRF-2008-357-D00103]. Supporting Information is available online from Wiley InterScience or from the author.

Received: July 22, 2009
Revised: October 17, 2009
Published online: December 28, 2009

[1] a) K. Nomura, H. Ohta, A. Takagi, T. Kamiya, M. Hirano, H. Hosono, *Nature* **2004**, *432*, 488. b) H. Yabuta, M. Sano, K. Abe, T. Aiba, T. Den, H. Kumoni, K. Nomura, T. Kamiya, H. Hosono, *Appl. Phys. Lett.* **2006**, *89*, 112123. c) H. Q. Chiang, J. F. Wager, R. L. Hoffman, J. Jeong, D. A. Keszler, *App. Phys. Lett.* **2005**, *86*, 013503. d) N. L. Dehuff, E. S. Kettenring, D. Hong, H. Q. Chiang, J. F. Wager, R. L. Hoffman, C. H. Park, D. A. Keszler, *J. Appl. Phys.* **2005**, *97*, 064505. e) T. Moriga, D. R. Kammler, T. O. Mason, *J. Am. Ceram. Soc.* **1999**, *82*, 2705. f) H. S. Kim, M.-G. Kim, Y.-G. Ha, M. Kanatzidis, T. J. Marks, A. Facchetti, *J. Am. Chem. Soc.* **2009**, *131*, 10826.

[2] a) N. F. Mott, *Adv. Phys.* **1977**, *26*, 363. b) H. Hosono, *J. Non-Cryst. Solids* **2006**, *352*, 851. c) S. Narushima, K. Ueda, H. Mizoguchi, H. Ohta, M. Hirano, K. Shimizu, T. Kamiya, H. Hosono, *Adv. Mater.* **2003**, *15*, 1409.

[3] a) K. Nomura, A. Takagi, T. Kamiya, H. Ohta, M. Hirano, H. Hosono, *Jpn. J. Appl. Phys.* **2006**, *45*, 4303. b) K. Nomura, T. Kamiya, H. Ohta, T. Uruga, M. Hirano, H. Hosono, *Phys. Rev. B* **1996**, *54*, 11169.

[4] A. K. Varshneya, *Fundamentals of Inorganic Glasses*, Academic Press, Inc., New York **1993**.

[5] a) E. M. C. Fourtunato, L. M. N. Pereira, P. M. C. Barquinha, A. M. Bothlho do Rego, G. Gonçalves, A. Vilà, J. R. Morante, R. F. P. Martins, *Appl. Phys. Lett.* **2008**, *92*, 222103. b) M. Kim, J. Ho. Jeong, H. J. Lee, T. K. Ahn, H. S. Shin, J.-S. Park, J. K. Jeong, Y.-G. Mo, H. D. Kim, *Appl. Phys. Lett.* **2007**, *90*, 212114. c) Y.-L. Wang, F. Ren, W. Lim, D. P. Norton, S. J. Pearton, I. I. Kravchenko, J. M. Zavada, *Appl. Phys. Lett.* **2007**, *90*, 232103. d) P. Görrn, P. Hölzer, T. Riedl, W. Kowalsky, J. Wang, T. Weimann, P. Hinze, S. Kipp, *Appl. Phys. Lett.* **2007**, *90*, 063502. e) B. Yaglioglu, H. Y. Yeom, R. Beresford, D. C. Paine, *Appl. Phys. Lett.* **2006**, *89*, 062103. f) W. B. Jackson, R. L. Hoffman, G. S. Herman, *Appl. Phys. Lett.* **2005**, *87*, 193503.

[6] a) G. Thomas, *Nature* **1997**, *389*, 907. b) J. F. Wager, *Science* **2003**, *300*, 1245.

[7] a) S. Jeong, Y. Jeong, J. Moon, *J. Phys. Chem. C* **2008**, *112*, 11082. b) S.-J. Seo, C. G. Choi, Y. H. Hwang, B.-S. Bae, *J. Phys. D: Appl. Phys.* **2009**, *42*, 035106. c) C. G. Choi, S.-J. Seo, B.-S. Bae, *Electrochem. Solid-State Lett.* **2008**, *11*, H7. d) Y.-J. Chang, D.-H. Lee, G. S. Herman, C.-H. Chang, *Electrochem. Solid-State Lett.* **2007**, *10*, H135. e) D.-H. Lee, Y.-J. Chang, G. S. Herman, C.-H. Chang, *Adv. Mater.* **2007**, *19*, 843.

[8] K. Nomura, A. Takagi, T. Kamiya, H. Ohta, M. Hirano, H. Hosono, *Jpn. J. Appl. Phys.* **2006**, *45*, 4503.

[9] a) K. H. Kim, G. H. Kim, H. S. Shin, B. D. Ahn, S. Kang, H. J. Kim, *Electrochem. Solid-State Lett.* **2008**, *155*, H848. b) G. H. Kim, H. S. Shin, B. D. Ahn, K. K. Kim, W. J. Park, H. J. Kim, *Electrochem. Solid-State Lett.* **2009**, *156*, H7. c) G. H. Kim, B. D. Ahn, H. S. Shin, W. H. Jeong, H. J. Kin, H. J. Kim, *Appl. Phys. Lett.* **2009**, *94*, 233501.

[10] a) J. C. C. Fan, J. B. Goodenough, *J. Appl. Phys.* **1997**, *48*, 3524. b) S. Major, S. Kumar, M. Bhatnagar, K. L. Chopra, *Appl. Phys. Lett.* **1986**, *49*, 394. c) T. Ishida, H. Kobayashi, Y. Nakato, *J. Appl. Phys.* **1993**, *73*, 4344.

[11] H. Hosono, *J. Non-Cryst. Solids* **2006**, *352*, 851.

[12] T. Iwasaki, N. Itagaki, T. Den, H. Kumomi, K. Nomura, T. kamiya, H. Hosono, *Appl. Phys. Lett.* **2007**, *90*, 242114.

[13] a) H. Hosono, K. Nomura, Y. Ogo, T. Uruga, T. Kamiya, *J. Non-Cryst. Solids* **2008**, *354*, 2796. b) K. Nomura, T. Kamiya, H. Yanagi, E. Ikenaga, K. Yang, K. Kobayashi, M. Hirano, H. Hosono, *Appl. Phys. Lett.* **2008**, *92*, 202117. c) M. Kimura, T. Kakanishi, K. Nomura, T. Kamiya, H. Hosono, *Appl. Phys.*

Lett. **2008**, *92*, 133512. d) K. Nomura, T. Kamiya, H. Ohta, K. Shimizu, M. Hirano, H. Hosono, *Phys. Status Solidi A* **2008**, *205*, 1910.

[14] a) S. T. Meyers, J. T. Anderson, C. M. Hung, J. Thompson, J. F. Wafer, D. Keszler, *J. Am. Chem. Soc.* **2008**, *130*, 17603. b) L. Wang, M.-H. Yoon, A. Facchetti, T. J. Marks, *Adv. Mater.* **2007**, *19*, 3252. c) L. Wang, M.-H. Yoon, G. Lu, A. Facchetti, T. J. Marks, *Nat. Mater.* **2006**, *5*, 893. d) C. Li, Y. Li, Y. Wu, B.-S. Ong, R.-O. Loutfy, *J. Mater. Chem.* **2009**, *19*, 1626. e) B. S. Ong, C. Li, Y. Li, Y. Wu, R. Loutfy, *J. Am. Chem. Soc.* **2007**, *129*, 2750. f) H. S. Kim, P. D. Byne, A. Facchetti, T. J. Marks, *J. Am. Chem. Soc.* **2008**, *130*, 12580.